Available online at www.sciencedirect.com

ScienceDirect

IFAC Papers Online CONFERENCE PAPER ARCHIVE

IFAC PapersOnLine 50-1 (2017) 4528–4533

Boundary control of a Rijke Tube using irrational transfer functions with experimental validation

Gustavo A. de Andrade * **Rafael Vazquez** ** **Daniel J. Pagano** *

* *Department of Automation and Systems, Universidade Federal de Santa Catarina, 88040-900, Florianópolis, SC, Brazil (e-mail: gustavo.artur@posgrad.ufsc.br, daniel.pagano@ufsc.br)*

** *Department of Aerospace Engineering, Universidad de Sevilla, Camino de los Descubrimientos, s.n.,41092 Sevilla, Spain (e-mail: rvazquez1@us.es)*

Abstract: This paper is concerned with boundary stabilization of thermoacoustic oscillations in the Rijke tube. This system consists of a vertical tube open in both ends and a heater placed in the lower half of the tube. A speaker placed under the tube is used as actuator while a microphone placed near the top of the tube provides the pressure measurement. To study this problem we consider that the mathematical model takes the form of two interconnected compartments: one for the cold zone and other for the hot zone. The control input is applied on the left boundary condition of the cold zone. From this model we derive an irrational transfer function to design a stabilizing boundary control in the frequency domain. In particular, we derive necessary and sufficient conditions for the input-output stability through the use of Nyquist-type test. Experimental results show the effectiveness and real-life applicability of the method.

Keywords: Partial differential equations, stabilization, Frequency domain, Irrational transfer functions, Nyquist stability criterion, Thermoacoustic oscillations

1. INTRODUCTION

In this paper, we investigate boundary stabilization of thermoacoustic oscillations. First a theoretical model is rigorously studied to obtain stabilizing control laws, which are later tested in an experimental setting. The phenomenon of thermoacoustic oscillations is described by high levels of sound produced due to the feedback between heat release rate fluctuations and acoustic pressure fluctuations in confined spaces.

The Rijke tube serves as a convenient prototype system to study thermoacoustic phenomena. A Rijke tube is a vertical tube, typically made of glass, open on both ends and with a heating element placed towards the lower end. A speaker, placed at a slight distance under the tube, is used as actuator, and a microphone located near the top of the tube is used as sensor. The mathematical model of the Rijke tube take a form of two interconnected compartments: a cold zone below the heater and a hot zone above it. These parts are given by the Euler equations of gas dynamics. The heater is introduced as an interaction between the pressure and velocity field of these components. Furthermore, the control variable is considered as a boundary condition for the pressure in cold zone. Depending on the steady-state conditions about which the Euler equations are linearized, the resulting linearization is a linear first-order partial differential equation (PDE) that behaves like a wave equation and thus describes acoustic wave propagation (de Andrade et al., 2016). The linearization of this model leads to the system considered throughout this paper.

Many authors contributed to the control of thermoacoustic instabilities. The contributions range from phase shift controllers (Heckl, 1988) to LQG controllers (Murugappan et al., 2003) or H_∞ robust controllers (Campos-Delgado et al., 2003). Most of these works use a finite dimensional approximation of the system to design controllers. Recent approaches took into account distributed feature of the system, for example either by using a PI controller (Krstic et al., 1999), or by a Riemann invariant approach (de Andrade et al., 2016).

In this work we consider a control methodology based on a frequency domain approach. Starting from the linearized PDE system in a steady-state regime, we apply the Laplace transform to consider the linearized PDE in the frequency domain, and classical frequency domain tools are used to design the controller in a similar way as for systems represented by rational transfer functions. Our objective in this paper is to consider this approach with a rigorous perspective, and to show what can effectively be guaranteed by using such a frequency domain approach for the

⋆ This work has been partially funded by the following projects: MTM2015-65608-P financed by Spanish Ministerio de Economía y Competitividad and by CNPq-BRASIL under the grant 438387/2016-3.

10.1016/j.ifacol.2017.08.726

Rijke tube by considering an infinite dimensional model. Moreover, we test the proposed control methodology in a experimental setup to show its effectiveness and real-life applicability of the method.

The paper is organized as follows. Section 2 presents the description of thermoacoustic oscillations, the Rijke tube, its linearized mathematical model and the characterization of the transfer function. The closed loop system and its stability is studied in Section 3. The experimental results are shown in Section 4. Finally, the main conclusions are presented in Section 5.

Notation The set of real numbers is denoted by $\mathbb{R}$. The set of positive integers is denoted by $\mathbb{N}$. We denote $\mathbb{C}$ as the set of complex numbers and $\overline{\mathbb{C}^+}$ all complex numbers with real part larger than or equal zero. By s we denote the complex variable, that is, $s = \sigma + j\omega$, with σ and ω real numbers and $j^2 = -1$. By $\mathbf{H}_\infty$, we denote the Hilbert space $\mathbf{H}_\infty = \{u : \overline{\mathbb{C}^+} \to \mathbb{C} |\, u \text{ analytic and } \sup_{Re(s)>0} |u(s)| < \infty\}$, with norm $\|u\|_\infty = \sup_{Re(s)>0} |u(s)|$. The Hilbert space of measurable and square integrable $\mathbf{L}^2$-functions is denoted by $\mathbf{L}_2(0, \infty) = \left\{u : [0, \infty) \to \mathbb{C} |\, \int_0^\infty |u(t)|^2 dt < \infty\right\}$, with the $\mathbf{L}_2$-norm $\|u\|_2 = \left(\int_0^\infty |u(t)|^2\right)^{1/2}$. The class of continuously differentiable functions from $[a, b]$ to $\mathbb{R}^n$ is denoted by $C^1([a, b]; \mathbb{R}^n)$.

2. SYSTEM DESCRIPTION

2.1 The Rijke tube

In this work, all the experiments were performed on a simple 1.3 meter long glass tube with an electrical heating element made of nichrome wire coil. The power is delivered into the coil using a DC power supply with power output 360 W. The location of the electrical heating element was chosen to be a quarter of the tube length. The sound pressure in the tube is measured with a clip-on microphone with built-in preamplifier. This signal is sent to a control computer through a data acquisition device. The control system is implemented as part of a SCADA program based on a LabVIEW software. In such configuration the control algorithm is implemented as a Matlab function executed from the SCADA program. For the closed-loop experiments it was used a 30 W ceiling speaker as the actuator together with a linear amplifier. A schematic of the Rijke tube is depicted in Figure 1.

2.2 The thermoacoustic phenomenon

In the Rijke tube, the heat source transfer heat to the air in the tube, making the air to rise up and creating an upward flow. The rising hot air becomes dense by coming in contact with the cooler walls of the upper half of the tube. This means that in the lower half of the tube, the air always experiences expansion, while in the upper part, the air always experience compression. Moreover, according to the Rayleigh's criterion (Rayleigh, 1945), a standing pressure wave is sustained if heat is added during condensation, or be taken from it at the moment of rarefaction. On the other hand, if heat is added during rarefaction, or

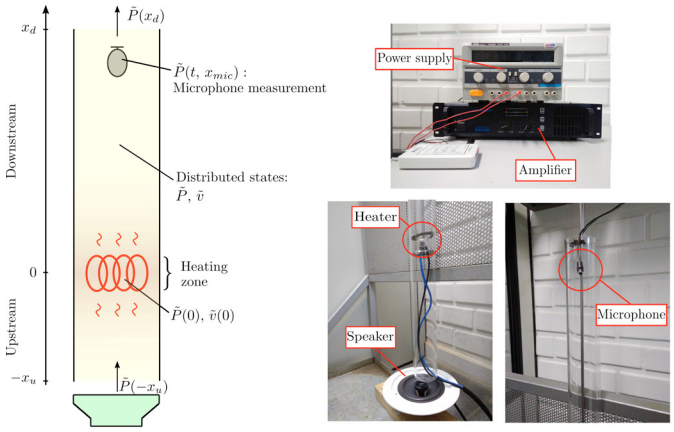

Fig. 1. Rijke tube schematic.

abstracted at the moment of condensation, the pressure wave is discouraged. In mathematical terms, the Rayleigh's criterion is formulated in terms of the Rayleigh integral over the control volume V given by

$$I = \oint_V \tilde{P}(t)\tilde{Q}(t)dt, \tag{1}$$

where $\tilde{P}$ is the acoustic pressure fluctuation, $\tilde{Q}$ is the fluctuation of heat power released in the heater, and t is time. According to the Rayleigh's criterion, if $I < 0$, the pressure wave will be damped. If $I > 0$, then the pressure wave will grow. Otherwise, if $I = 0$, the pressure wave will neither be damped out nor amplified.

2.3 Mathematical model

The Rijke tube can be modeled as a heating section embedded within a network of pipes. We assume that the fluctuations of pressure and velocity occur only along the axial direction. Therefore, the system can be described by the one-dimensional mathematical model of compressible gas dynamics. Furthermore, the heating release zone is assumed to be located in a very narrow section.

The Rijke tube is composed of 2 compartments described by the linearized Euler equations of gas dynamics:

$$\partial_t \tilde{v}_i(t, x_i) + \frac{1}{\overline{\rho}} \partial_{x_i} \tilde{P}_i(t, x_i) = 0, \tag{2}$$

$$\partial_t \tilde{P}_i(t, x_i) + \gamma \overline{P} \partial_{x_i} \tilde{v}_i(t, x_i) = 0, \tag{3}$$

$$i = 1, 2,$$

where $t \in [0, +\infty)$ is the time, $x_1 \in (-x_u, 0)$, $x_2 \in (0, x_d)$, $x_u, x_d > 0$, γ is the adiabatic ratio, $\tilde{P}$ is the pressure fluctuation, and $\tilde{v}$ is the velocity fluctuation. The steady-state density and pressure are denoted by $\overline{\rho}$ and $\overline{P}$, respectively. It is important to emphasize that in this work the steady-state density, pressure and velocity are assumed to be constant along the space. Furthermore, the steady-state values are considered the same for both compartments of the tube.

The initial condition is defined by

$$\tilde{v}_i(0, x_i) = \tilde{v}_{i,0}(x_i), \qquad \tilde{P}_i(0, x_i) = \tilde{P}_{i,0}(x_i),$$
$$i = 1, 2.$$

We represent the interconnection between the downstream and upstream part of the system by the following algebraic

relations, which can be directly obtained by linearizing the equations conservation of mass, momentum and energy across the heat zone $x = 0$,

$$\tilde{P}_2(t,\,0) + \overline{\rho v}\tilde{v}_2(t,\,0) - \tilde{P}_1(t,\,0) - \overline{\rho v}\tilde{v}_1(t,\,0) = 0, \quad (4)$$

$$\frac{\gamma}{\gamma-1}\overline{v}\tilde{P}_2(t,\,0) + \left(\frac{\gamma}{\gamma-1}\overline{P} + \overline{\rho v^2}\right)\tilde{v}_2(t,\,0) - \frac{\gamma}{\gamma-1}\overline{v}\tilde{P}_1(t,\,0) - \left(\frac{\gamma}{\gamma-1}\overline{P}_1 + \overline{\rho v^2}\right)\tilde{v}_1(t,\,0) = \frac{\tilde{Q}}{A}(t), \quad (5)$$

where A is the cross-sectional area of the tube and $\tilde{Q}$ is the fluctuation of heat power released in the heater. Following Epperlein et al. (2015), we assume that the fluctuation of heat power is expressed by the following ordinary differential equation (ODE)

$$t_{hr}\tilde{Q}'(t) = -\tilde{Q}(t) + h_v\tilde{v}_1(t,0), \quad (6)$$

where t_{hr} is the heat release time constant and h_v is the velocity-dependent heat transfer coefficient.

Moreover, the system (2)-(3) is subjected to the following boundary conditions

$$\tilde{P}_1(t,-x_u) = U(t), \qquad \tilde{P}_2(t,x_d) = 0, \quad (7)$$

where U is the control input.

The operational parameters used in this paper are shown in Table 1.

Remark 1. In Heckl (1988) it was computed an explicit estimation for the Rayleigh integral (1) from the equations (2)-(7). The thermoacoustic oscillations amplitude grows if the acoustic energy stored in the tube increases in time average, i.e.,

$$\frac{\gamma-1}{\overline{\rho}c^2}\overline{\tilde{P}(0)}\frac{\overline{Q}}{A} > \overline{\tilde{P}(L)}\overline{\tilde{v}(L)} - \overline{\tilde{P}(0)}\overline{\tilde{v}(0)} + \eta Lc\left(\frac{\overline{\tilde{P}^2(0)}}{\overline{\rho}c^2} + \overline{\rho}\overline{\tilde{u}^2(0)}\right), \quad (8)$$

where $\overline{\bullet}$ is the mean value (in time) of its argument, $\eta Lc\left(\frac{\overline{\tilde{P}^2(0)}}{\overline{\rho}c^2} + \overline{\rho}\overline{\tilde{u}^2(0)}\right)$ is the Stokes layer, and η is the attenuation constant of the sound wave traveling along the tube.

Well-posedness Without loss of generality, it can be assumed that, by re-scaling the space variable, the two counterparts of PDE (2)-(3) evolve in the domain from 0 to 1. Furthermore, in this framework it can be assumed that there are only coupling at the boundaries between themselves. This leads to express the system (2)-(7) into

$$\begin{aligned} &\partial_t\xi(t,\,z) + \mathbf{A}\partial_z\xi(t,\,z) = 0,\\ &\xi(0,\,t) = \xi_0(z),\\ &g_L(\xi(t,\,z),\,U(t)) = 0, \qquad g_R(\xi(t,\,1)) = 0, \end{aligned} \quad (9)$$

where $\xi = (\tilde{P}_1,\,\tilde{v}_1,\,\tilde{P}_2,\,\tilde{v}_2)$, $z \in [0,\,1]$ is the re-scaled space variable, g_L and g_R are the left and right boundary conditions, ξ_0 is the initial condition and $\mathbf{A}$ is a matrix with real coefficients. We omit the explicit expression of $\mathbf{A}$, g_L and g_R due to lack of space.

The existence and uniqueness of the solution of system (9) can be proved by the method of characteristics, which enables us to restate the PDE as a set of classical ODEs. Then, if ξ_0 and U are continuously differentiable functions of their arguments and if ξ_0 and the boundary conditions verify conditions of C^1 compatibility, one can show that the solutions of the system are continuously differentiable with respect to their arguments, i.e., $\xi \in C^1([0,\,1]\times[0,\,\infty);\mathbb{R}^4)$. Moreover, based on an extension of Litrico and Fromion (2009), there exist $M > 0$ and η such that for any $t \in [0,\infty)$, any $\xi \in C^1([0,\,1];\mathbb{R}^6)$ and any $U^{(t)} \in \mathbf{L}^2([0,\,t];\mathbb{R}^4) \cap C^1([0,\,t],\mathbb{R}^4)$, there exists K_t such that

$$\|\xi(\cdot,t)\|_{\mathbf{L}^2([0,\,1];\mathbb{R}^4)} + \left|\tilde{Q}(t)\right| \le Me^{\eta t}\left(\|\xi_0\|_{\mathbf{L}^2([0,\,1];\mathbb{R}^4)} + \left|\tilde{Q}(0)\right|\right) + K_t\left\|U^{(t)}\right\|_2,$$

where $U^{(t)}$ denotes the restriction of U to $[0,\,t]$.

Table 1. Values of the parameters of the system.

Symbol	Description	Value
$\overline{\rho}$	Density	1.2 kg/m^3
$\overline{P}$	Pressure	10^5 N/m^2
$\overline{v}$	Velocity	0.35 m/s
γ	Adiabatic ratio	1.4
$\overline{\gamma}$	-	0.4
L	Tube length	1.3 m
x_0	Heater position	$\frac{1}{4}L$
d	Tube diameter	0.0762 m
R_u	Reflection coefficient	-0.95
R_d	Reflection coefficient	-0.95
t_{hr}	Heat-release time constant	0.002
h_v	Velocity-dependent heat transfer coefficient	200

2.4 Open-loop transfer function

The well-posedness of the solution enables us to use a frequency domain approach. We start by applying the Laplace transform to (2)-(7) in order to obtain a transfer function $G(s)$ from the speaker to the microphone pressure. To derive this transfer function, note that equations (2)-(3) represent the wave equation. To see that, take both a time and space derivative in (3) and subtract the resulting expressions. One obtains

$$\partial_{tt}\tilde{P}_i(t,\,x_i) = c^2\partial_{x_ix_i}\tilde{P}_i(t,\,x_i), \qquad i = 1,\,2, \quad (10)$$

where $c = \sqrt{\gamma\frac{\overline{P}}{\overline{\rho}}}$ is the speed of sound.

It is well known that the solution of (10) is given by the d'Alambert formula (Evans, 2010). Therefore, the acoustic pressure in the upstream propagates according to

$$\tilde{P}_1(t,x) = f\left(t - \frac{x}{c}\right) + g\left(t + \frac{x}{c}\right), \quad -x_u < x < 0, \quad (11)$$

and similarly to the downstream side

$$\tilde{P}_2(t,x) = h\left(t - \frac{x}{c}\right) + j\left(t + \frac{x}{c}\right), \quad 0 < x < x_d, \quad (12)$$

where f, g, h, j are functions which satisfy the boundary and initial conditions.

Substituting (11)-(12) into (2) and integrating over time, we get the expression of the velocity fluctuations at the upstream and downstream part of the tube:

$$\tilde{v}_1(t,x) = \frac{1}{\bar{\rho}c}\left(f\left(t-\frac{x}{c}\right) - g\left(t+\frac{x}{c}\right)\right), \quad -x_u < x < 0, \tag{13}$$

$$\tilde{v}_2(t,x) = \frac{1}{\bar{\rho}c}\left(h\left(t-\frac{x}{c}\right) - j\left(t+\frac{x}{c}\right)\right), \quad 0 > x > x_d. \tag{14}$$

From the boundary conditions (7), we get $f(t) = -g\left(t-2\frac{x_u}{c}\right) + U(t-\frac{x_u}{c})$ and $j(t) = -h\left(t-2\frac{x_d}{c}\right)$. These reflections at tube ends are modeled for ideal condition. A more realistic model should include acoustic reflection losses at the boundary. Therefore, we introduce the constants $R_u, R_d \in (-1, 0)$ to account for acoustic reflection losses. It follows that these boundary conditions are rewritten to

$$f(t) = R_u g\left(t-\tau_u\right) + U\left(t-\frac{\tau_u}{2}\right), \tag{15}$$

$$j(t) = R_d h\left(t-\tau_d\right), \tag{16}$$

where $\tau_u = 2\frac{x_u}{c}$ and $\tau_d = 2\frac{x_d}{c}$.

The open-loop transfer function required, $G(s)$, is from the speaker to the microphone pressure. This can be obtained by considering $x = 0$ and substituting (11)-(16) into (4)-(5), and applying the Laplace transform into these equations. After some algebraic manipulations we obtain the final expression for the required transfer-function:

$$G(s) = \frac{\mathcal{P}_{mic}(s)}{\mathcal{U}(s)} = -\frac{2e^{-\left(\frac{x_u+x_{mic}}{c}\right)s}}{(\gamma-1)\det(\mathbf{S})}\times \left(1+R_d e^{2\left(\frac{x_{mic}-x_d}{c}\right)s}\right)(1+(\gamma-1)\phi(s)), \tag{17}$$

where $\mathcal{P}_{mic}$ and $\mathcal{U}$ are the Laplace transform of $\tilde{P}_2(t,\, x_{mic})$ and U, respectively, $x_{mic} \in (0, x_d)$ is the location of the microphone, $\phi(s) = \frac{h_v}{t_{hr}s+1}$ and

$$\mathbf{S} = \begin{pmatrix} -1-R_u e^{-\tau_u s} & 1+R_d e^{-\tau_d s} \\ \dfrac{(1-R_u e^{-\tau_u s})}{\gamma-1}(1+(\gamma-1)\phi(s)) & \dfrac{1-R_d e^{-\tau_d s}}{\gamma-1} \end{pmatrix}.$$

Poles of the open-loop system The poles of $G(s)$ characterize the open-loop dynamic behavior of the linearized system. They are given by the solutions of the following equation:

$$\psi(s) \triangleq (1-R_d e^{-\tau_u s})(1-R_d e^{-\tau_d s}) - (1-R_u e^{-\tau_u s})(\tau s + 1 + (\gamma-1)h_v)(1+R_d e^{-\tau_d s}) = 0. \tag{18}$$

In general, this equation has no explicit solution. Numerical resolution for the values in Table 1 leads to the poles depicted in Figure 2. As can be seen, there is a pair of unstable complex conjugated poles at the frequency 131 Hz, and infinite poles on the left hand side of the complex plane. The following proposition provides a closed solution of (18) to explain the poles behavior for high frequency, in which the proof was omitted due to lack of space.

Proposition 2. When $|s| \gg 0$, the solutions of (18) tend asymptotically towards

$$\tilde{p}_{\pm k} = \frac{\log(R_u R_d)}{\tau_u+\tau_d} \pm \frac{2j\pi k}{\tau_u+\tau_d}, \tag{19}$$

where $k \in \mathbb{N}$, and the approximation error is at the first-order given by:

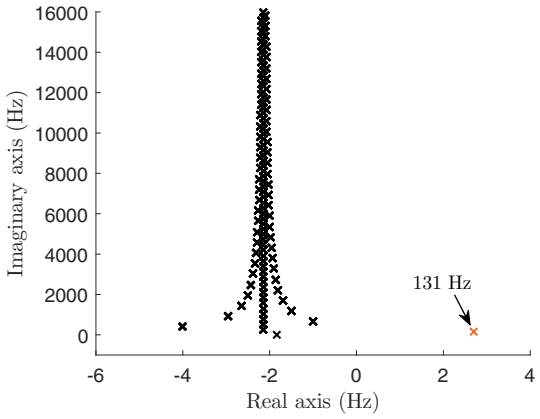

Fig. 2. Location of the poles of the open-loop transfer function (17). They were calculated numerically by finding roots of (17). Note that there is an unstable pole at 131 Hz, and infinite stable poles that tend asymptotically towards (19).

$$p_{\pm k} \approx \tilde{p}_{\pm k} - \frac{\psi(\tilde{p}_{\pm k})}{\psi'(\tilde{p}_{\pm k})}. \tag{20}$$

Figure 3 shows the open-loop frequency response for the model (17) and the real experiment described in Section 2 over the frequency range $100 - 900$ Hz. As can be seen, by comparing Figure 3(a) and Figure 3(b), the response of the irrational transfer function (17) and the real system are very similar in the frequency range of interest.

3. CLOSED-LOOP SYSTEM

3.1 Proposed control law

As shown in Equation (8), the thermoacoustic oscillation in the Rijke tube occurs when acoustic energy is greater than the loss. The gain and loss of energy depend on the acoustic field. However, conditions can change completely if the field in the tube is disturbed by a different sound source, which in this work is produced by a loudspeaker. The inclusion of a sound source changes the difference between energy gain and loss, which can become larger or smaller than the unperturbed acoustic field. Therefore, it is reasonable to consider the control law given by

$$u(t) = K_c \tilde{P}(t-\tau_c, x_{mic}), \tag{21}$$

where K_c and τ_c are design parameters. Note that with this control law the loudspeaker reproduces an amplified and delayed pressure wave of the tube.

3.2 Stability analysis

In this work, the following definition of stability is adopted.

Definition 3. If a system maps every input u in $\mathbf{L}_2(0,\, \infty)$ to an output y in $\mathbf{L}_2(0,\, \infty)$ and

$$\sup_{u\neq 0} \frac{\|y\|_2}{\|u\|_2} < \infty,$$

the system is stable. A system is said to be unstable if it is not stable.

Remark 4. Stability of systems described by their transfer functions can be checked by Theorem A.2 of Curtain and Morris (2009). In this case, a linear system is stable if and only if its transfer function G belongs to $\mathbf{H}_\infty$.

With control law (21), the closed-loop transfer function is given by

$$G_{cl}(s) = \frac{G(s)}{1 - C(s)G(s)}, \tag{22}$$

where $C(s) = K_c e^{-\tau_c s}$.

For the stability result we will use the following necessary and sufficient condition (Desoer and Vidyasagar, 1975).

Theorem 5. The closed-loop system is stable if and only if

(1) $\inf_{\mathrm{Re}(s)>0} |1 - C(s)G(s)| > 0$
(2) $C(p_i) \neq 0, \quad i = 1, \ldots, n_0$, where p_i are the poles of G in $\overline{\mathbb{C}^+}$.

Condition 1 of Theorem 5 can be checked through the graphic Nyquist criteria. In our case, the open-loop is non strictly proper, and the application of the graphic Nyquist criteria is more delicate (Desoer and Vidyasagar, 1975). Condition 2 of the previous theorem corresponds to a condition preventing an instability due to the cancellation of an unstable pole of G by a zero of C.

Since the proposed control law (21) is not strictly proper, we have to take into account the behavior of the Nyquist plot at infinity. We propose below a way to circumvent this problem by analyzing the closed-loop poles for high frequencies. First, consider that the system fulfills the following assumption

Assumption 6. The set

$$r = \{x_u + x_d,\, c\tau_c + x_d + x_{mic},\, c\tau_c + 3x_d - x_{mic}\},$$

is rationally independent [1].

Then, using Theorem 2.2 and Corollary 2.4 of Hale and Lunel (2002) we have the following necessary condition of stability:

Proposition 7. Let τ_c, $x_{mic} > 0$ such that

$$r = (x_u + x_d,\, c\tau_d + x_d + x_{mic},\, c\tau_c + 3x_d - x_{mic}),$$

is rationally independent. Then, the following inequality is a necessary condition of closed-loop stability:

$$|K_c|(1 + |R_d|) < 1 - R_d R_u \tag{23}$$

Proof. For $|s| \gg 0$, the closed-loop poles can be approximated as the solution of

$$1 - R_u R_d e^{-(\tau_u+\tau_d)s} - K_c e^{-\left(\frac{c\tau_c + x_d + x_{mic}}{c}\right)s} - K_c R_d e^{-\left(\frac{c\tau_c + 3x_d - x_{mic}}{c}\right)s} = 0. \tag{24}$$

Then, choosing τ_c, $x_{mic} > 0$ such that

$$r = (x_u + x_d,\, c\tau_d + x_d + x_{mic},\, c\tau_c + 3x_d - x_{mic}),$$

is rationally independent we can apply Theorem 2.2 and Corollary 2.4 of (Hale and Lunel, 2002) to obtain the inequality (23). This concludes the proof.

Using this result we can restrict the test of the Nyquist criterion to a finite range of frequencies, as stated in the corollary bellow.

Corollary 8. If Proposition 7 is verified, then there exists $s_0 > 0$ such that condition 1 of Theorem 5 needs only be tested on a finite range $|s| < s_0$.

The version of the Nyquist theorem which accomodates infinite dimensional systems can be seen in Theorem A.1.14 of Curtain and Zwart (1995). In the next proposition we show the conditions that the Nyquist contour must obey in this finite range of frequencies in order to guarantee the stability of the closed loop system.

Proposition 9. Let n_u be the number of open-loop poles of (17) in $\overline{\mathbb{C}^+}$. Denote the Nyquist contour of

$$\Psi(s) \triangleq 1 + \frac{2K_c e^{-\left(\frac{c\tau_c + x_u + x_{mic}}{c}\right)s}}{(\gamma - 1)\det(\mathbf{S})}(1 + R_d e^{2\left(\frac{x_{mic} - x_d}{c}\right)s}) \times (1 + (\gamma - 1)\phi(s)) \tag{25}$$

by $\Gamma_{\Psi(s)}$. Then the transfer function G_{cl} is

(1) Unstable if $\Gamma_{\Psi(s)}$ does not encircles the origin n_u times in the clockwise direction.
(2) Stable if $\Gamma_{\Psi(s)}$ encircles the origin n_u times in the clockwise direction.

In the limiting case that $\Gamma_{\Psi(s)}$ does not encircle but crosses -1, the stability is undetermined.

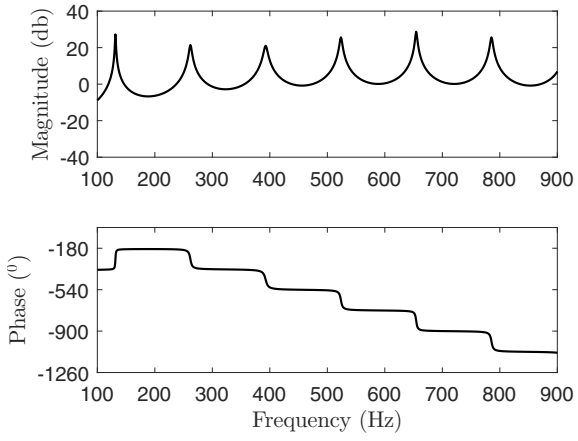

(a) Open-loop frequency response of model (17).

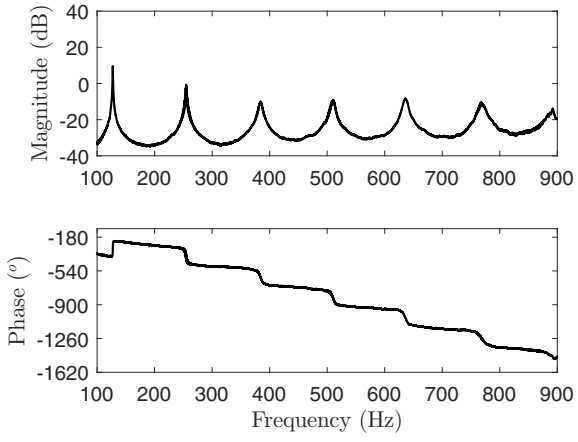

(b) Open-loop frequency response obtained by applying a sine sweep, over the range 100 − 900 Hz, into the real experimental plant.

Fig. 3. Open-loop frequency response of model (17) and the experimental plant.

[1] We say that the real numbers $a_1, \ldots, a_n$ are rationally independent if the only n-tuple of integers $k_1, \ldots, k_n$ such that $k_1 a_1 + \cdots + k_n a_n = 0$ is the trivial solution in which every k_i, $i = 1, \ldots, n$ is zero.

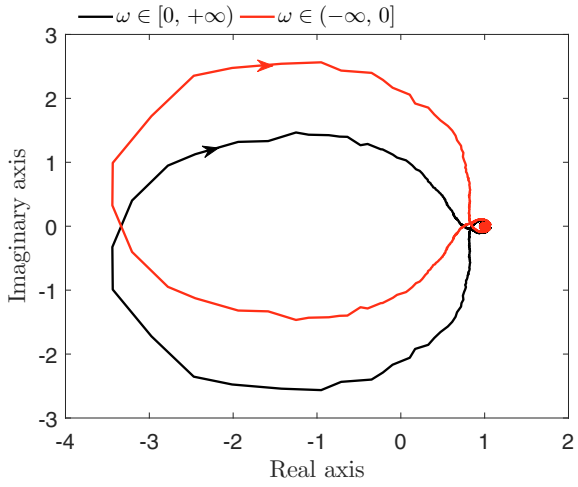

Fig. 4. Nyquist plot of $\Gamma_{\Psi(s)}$ showing two clockwise encirclements of the origin as ω decreases from $+\infty$ to $-\infty$. This graphic was obtained experimentally on the Rijke tube configuration described in Section 2.

We skip the proof of Proposition 9 since it follows from standard arguments.

In sum, the necessary and sufficient conditions developed in this section can be checked by the algebraic equation (23) and by choosing τ_c and x_{mic} such that Assumption 6 and the Nyquist criterion are satisfied.

4. EXPERIMENTAL RESULTS

In this section, we present results of experiments in the Rijke tube configuration described in Section 2 with control law (21). We choose $K_c = 0.002$ and τ_c was designed in order to $\Gamma_{\Psi(s)}$ encircles the origin twice in the clockwise direction since, as shown in Figure 3(b), the system has a pair of complex conjugate poles in $\overline{\mathbb{C}^+}$. The Nyquist plot of $\Gamma_{\Psi(s)}$ for $\tau_c = 0.001$ is depicted in Figure 4. There are two clockwise encirclements of the origin as ω decreases from $+\infty$ to $-\infty$.

Figure 5 shows the sound pressure at the microphone location and the control signal with the control law (21). At the beginning of the experiment, no controller is active, and the system is in the limit cycle. At $t = 3.5$ s the controller is activated. It can be noted that the oscillations are suppressed and the system remains in the operating point. At $t = 12$ s the control is deactivated and as expected, the system comes back to the oscillatory regime.

5. CONCLUSIONS

We have addressed the issue of boundary stabilization of thermoacoustic oscillations of the Rijke tube by a frequency domain approach. We have used some properties of the system transfer function to derive necessary and sufficient conditions for input-output stability of the boundary controlled system. Experimental results for a Rijke tube prototype shows the effectiveness of the approach.

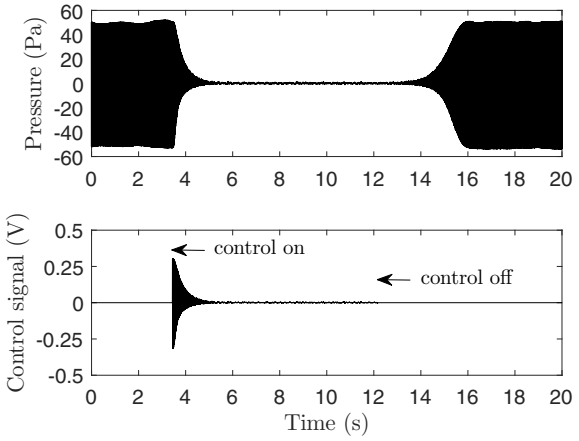

Fig. 5. Pressure fluctuations at the microphone location and control signal as a function of time. At $t = 3.5$ s the controller is actived. At $t = 12$ s the control is deactivated.

REFERENCES

Campos-Delgado, D.U., Schuermans, B.B.H., Zhou, K.M., Paschereit, C.O., Gallestey, E.A., and Poncet, A. (2003). Thermoacoustic instabilities: modeling and control. *IEEE Transactions on Control Systems Technology*, 11(4), 429–447.

Curtain, R. and Morris, K. (2009). Transfer functions of distributed parameter systems: A tutorial. *Automatica*, 45, 1101–1116.

Curtain, R.F. and Zwart, H.J. (1995). *An introduction to infinite-dimensional linear systems theory*. Springer Verlag, Berlin.

de Andrade, G., Vazquez, R., and Pagano, D.J. (2016). Boundary feedback control of unstable thermoacoustic oscillations in Rijke tube. In *Proceedings of the 2th IFAC Workshop on Control of Systems Governed by Partial Differential Equations*.

Desoer, C.A. and Vidyasagar, M. (1975). *Feedback systems: input output properties*. Academic Press, New York.

Epperlein, J.P., Bamieh, B., and Astrom, J. (2015). Thermoacoustics and the Rijke tube: Experiments, identification and modeling. *Control Systems Magazine*, 35(2), 57–77.

Evans, L.C. (2010). *Partial differential equations*. American Mathematical Society.

Hale, J.K. and Lunel, S.M.V. (2002). Strong stabilization of neutral functional differential equations. *IMA Journal of Mathematical Control and Information*, 19(1-2), 5–23.

Heckl, M.A. (1988). Active control of the noise from a Rijke tube. *Journal of Sound and Vibration*, 124(1), 117–133.

Krstic, M., Krupadanam, A., and Jacobson, C. (1999). Self-tuning control of a nonlinear model of combustion instabilities. *IEEE Transactions on Control Systems Technology*, 7(4), 424–436.

Litrico, X. and Fromion, V. (2009). Boundary control of hyperbolic conservation laws using a frequency domain approach. *Automatica*, 45, 647–656.

Murugappan, S., Acharya, S., Allgood, D.C., Park, S., Annaswamy, A.M., and Ghoniem, A.F. (2003). Optimal control of a swirl-stabilized spray combustor using system identification approach. *Combustion Science and Technology*, 175, 55–81.

Rayleigh, J.W.S. (1945). *The theory of sound*. Dover, New York.